An Experimental Framework for Validation of Thermal Modeling for Breast Cancer Detection

IOP Conf. Series: Materials Science and Engineering **408** (2018) 012031 doi:10.1088/1757-899X/408/1/012031

An Experimental Framework for Validation of Thermal Modeling for Breast Cancer Detection

Dastan Igali[1], Olzhas Mukhmetov[1], Yong Zhao[1,*], Sai Cheong Fok[1] and Soo Lee Teh[1]

[1] Department of Mechanical Engineering, School of Engineering, Nazarbayev University, Astana 010000, Republic of Kazakhstan

Email: yong.zhao@nu.edu.kz

Abstract. In recent years, breast cancer is considered as one of the most predominant causes of death among women in the world. This also accounts for the 11.7 % of the total cancers diagnosed among ladies in Kazakhstan. The survival chances of the patients can significantly be improved if the disease is detected at its earliest stage. At the present time, mammography is found to be the most common technique for the purpose of detecting the breast cancer. However, this method is very expensive, and the diagnostic ability of this imaging technique fails when it comes to the detection of tumours of small sizes, in addition to its harmful side effect. The IR thermography is inexpensive without any harmful side effect, and promises to be more precise than conventional techniques of detecting breast cancer at its earlier stage. In this study we propose a comprehensive method that includes FEM modelling based on heat transfer principles and requires 3D scanning and IR imaging for disease diagnosis. Here we report the first part of our study, which develops an experimental procedure to generate experimental results for the validation of FEM models for the simulation and detection of breast cancer.

1.Introduction

According to Francis et al [1], breast cancer is currently considered to be one of the most predominant causes of death among young women in the world. The annual mortality rate per 100,000 women from breast cancer in Kazakhstan has also increased by 9 % since 1990, an average of 0.39 % a year [2]. Sejtkazina et al. [3] claimed that breast cancer is the most commonly diagnosed cancer among ladies, representing about 11.7 % of the total cancers. As it has been reported, risk factors causing breast cancer include unfavourable living conditions, chronic stress which has become epidemic in our society, unilateral breastfeeding, breastfeeding less than 3 months or more than 2 years, abortions, and genetic predisposition[4]. Moreover, Bilyalova et al. [5] stated that there is a convincing evidence showing that breast cancer incidence in Kazakhstan varies with respect to ecological regions, thereby demonstrating higher mortality rates from this disease in areas with greater levels of contaminants in the atmosphere.

There are many other techniques of breast cancer detection, such as mammography, ultrasound and MRI. They mostly rely on finding the tumor physically and cannot identify pre-cancerous stage of the breast. X-rays scan readings are strongly dependent on the breast tissue density and hormonal changes and cannot give accurate results if these two markers are not at normal state. Presently mammography is found to be the most common technique for detecting breast cancer. However, the diagnostic ability of this imaging technique fails when it comes to the detection of tumors of small sizes. Thus, the

disease may not be brought under control at its earliest stage, leading to further growth. In addition, repeated mammography procedures expose the patient's body to very high levels of ionizing radiation [6].

Patients' chances of survival might be improved significantly if the disease is detected at its early stage, followed by proper prognosis and therapy [1]. Continuous efforts have been made in order to discover additional and safer diagnosis techniques for early tumor detection. One of such technique is thermography, which is applied to detect the abnormalities of thermal profiles in a breast [7]. It was reported by Gautherie et al. [8] that the tumor can be discovered 8-10 years ahead compared to mammography. IR imaging allows the identification of the presence of an early stage tumor by using the thermal signs of variation in blood vessels. Gautherie et al. [8] carried out a study, in which 1527 patients with abnormalities in their breast were under observation for 12 years. As these studies have shown, almost a half of the patients involved developed cancer within 5 years. It was concluded by the researchers that the risk for future development of breast cancer can only be recognized after examination of the thermal images of the breast for abnormalities. However, there are several factors which can affect the accuracy of the IR imaging procedure, such as asymmetrical breast temperature patterns, temperature stability, mental state, and menstrual cycle [9].

It was discovered that the surface temperature over the cancerous region is significantly higher than that of the region surrounding it. Accordingly, a variety of breast abnormalities can be determined by analyzing breast thermal images and the differences of absolute values of temperatures in a region of interest. Furthermore if there is temperature difference between the right and left breasts of more than 0.5 ℃, it can be indicative enough to establish an abnormal condition of the breast. Thus, the study of the asymmetrical temperature patterns between contra lateral breasts is widely employed for the detection of breast cancer. The use of thermal imaging technique demonstrates that the metabolic activity and blood circulation in cancerous tissues and their surroundings are at increased rate compared to clinically healthy breast tissues. The cancerous tumors need increased blood circulation in order to provide nutrients to their cells by from existing blood vessels, inactive vessels, and other ones. Thereafter, increase in the surface temperature of the breast can be observed after employing thermal imaging. High precision IR cameras and powerful computers are required in order to obtain very accurate and high-quality images of temperature changes. Early stages of breast cancer can also be detected, if the camera has enhanced thermal sensitivity and infrared resolution of less than 0.1 ℃ [9].

There are specific thermal features according to which thermographers analyze the thermogram for the presence of cancer. Almost in all cases the contralateral breast is considered as reference to which study refers when detecting cancer. As reported by Hoekstra [10], the following thermographic signs characterize the breast disease:

- Asymmetric and hyperthermic vascular features;
- Focal patterns with +2.5 ℃ temperature difference;
- Asymmetric and unusual vascular patterns with complex features;
- Asymmetric and diffuse hyperthermia with +2°C temperature difference patterns which involves a whole breast or peri-areolar area;
- Concentrated heat along abnormal breast region [11].

These features can also be observed from Figure 1, where the thermographic breast images are provided with distinguishable thermal patterns of healthy and abnormal breasts.

We propose an automated intelligent system that uses accurate 3D scanning, IR thermography and FEM thermal modeling for early detection of breast cancer. This can be achieved through reverse thermal modeling, during which the 3D scanning provides high precision breast geometry, IR thermography generates the breast surface temperature profiles and reverse FEM thermal modeling automatically searches for the location and size of the tumor if there is any. As a first step towards achieving this goal, we need to develop a standard experimental procedure whereby we can validate the FEM model and related simulation results.

The main purpose of this project is to establish such a procedure for FEM model validation for

future breast cancer detection, wherein silicone breasts with precision geometry are produced with simulated tumor and their temperature profiles are studied by using an infrared camera.

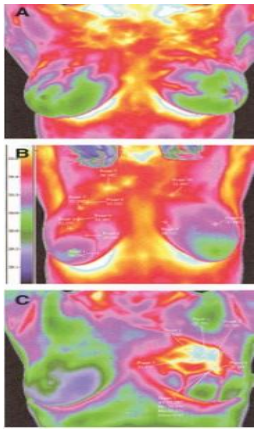

Figure 1. Thermographic breast images: (A) Clinically healthy breast; (B) Pre-cancerous stage of the breast; (C) Developed cancer in the left breast[11]

2. Methodology

2.1. 3D scanning

A 3D scanner, called ZScanner 700, is employed in this study. It is a unique self-positioning handheld device which makes 3D scanning process simple and efficient. It do not require any fixed-position tripods, mechanical arms and external positioning devices which complicates the scanning process of intricate or complex surfaces.

A female mannequin is used with accurate shape and size of a human body (see Figure 2). The mannequin has a height of 800 mm, chest of 838 mm, waist of 635 mm, which is scanned by the ZScanner 700. The breast region of the female mannequin was cut out for the study.

During scanning, positioning targets should be randomly affixed on the dummy breast with a distance of 30 mm between them (as seen in Figure 3). Those targets are required to define the position of the system in space. After the 3D image is obtained, the point cloud data is converted automatically into an STL file or polygon file or triangulated mesh. If further modifications are required (i.e. removal of unnecessary regions), the data can be further converted into CAD data (SLDPRT format).

Figure 2. Female mannequin

Figure 3. Breast region with targets

Figure 4 illustrates the scanned model with unnecessary regions removed. This image is now ready to be converted into CAD format and will be very used in future analysis. The dimensions of the 3D images are illustrated in the Figure 5 (in mm).

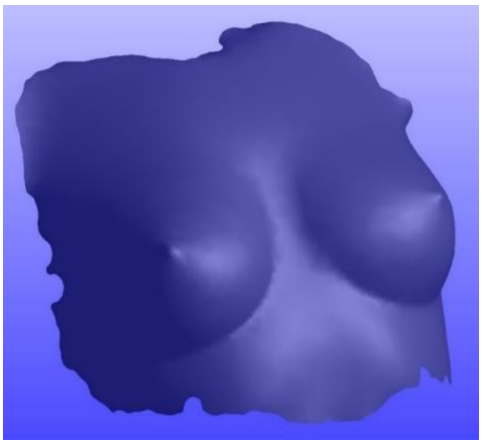

Figure 4. *Scan data with removed unnecessary parts*

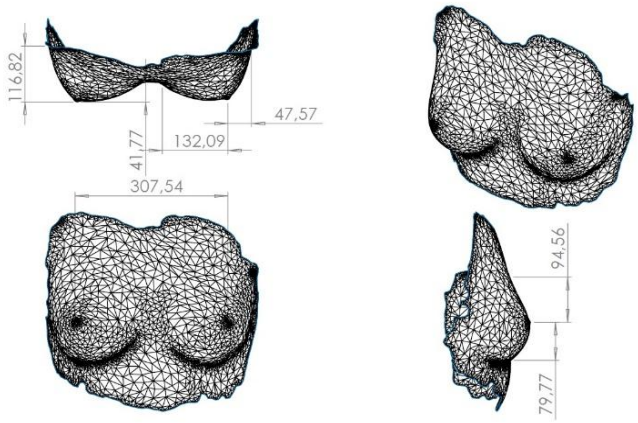

Figure 5. Orthographic projections of the breast

An infrared camera also known as a thermal-imaging camera is a device that measures the amount of infrared radiation falling on its infrared detector. Infrared camera operates at wavelengths roughly from 900 to 14,000 nm, while a simple camera can only operate in a range of 400-700 nm. Infrared image, after being transformed into radiometric one, can be viewed on a LCD screen where the user can observe temperature values. In this experiment, a thermographic camera called Fluke Ti29 is used to observe the temperature variations on the surface of the silicone breast. Fluke Ti29 cameras are able to detect small-scale temperature differences down to 0.1 degree. In addition, Fluke Ti29 has IT-fusion technology and blend modes which allow to display and store full visual images (640X480) and thermal images simultaneously. Thermal and visual images can be saved to a removable SD memory card and then transferred to a PC.

2.2. Resistors as heating elements for the simulation of tumors

Heat source for the experiment is made from several resistors connected very tightly in parallel and wires soldered from both sides to those resistors. Resistors produce heat as electric power is dissipated by them in a working circuit. Breast cancer is customarily associated with increases in the skin temperature around the tumor. Hence, heat sources consisting of resistors and wires are used to imitate the tumors' behaviors inside the real breast. Resistors used for this experiment are of the cylindrical shape with the length of 6 mm and diameter of 2 mm.

The volume of the resistor can be calculated as follows:

$$V = \pi r^2 h = \pi \times 1^2 \times 6 = 18.9\ mm^3$$

The volume of the heat source is determined by multiplying the volume of one resistor by the total number of resistors the heat source contains. Thus, the total volume of a heat source for each breast containing different number of resistors is provided in Table 1.

Table 1. The total volumes of heat sources for all the breasts

№	The total number of resistors in one heat source	Total volume, mm^3
1	4	75.4
2	8	150.8
3	6	113.1
4	4	75.4

In addition, the heat source of each breast is located differently, and their coordinates can be found in Table 2.

Table 2. Coordinates of heat sources

№	x, cm	y, cm	z, cm
1	9.2	8.9	3.5
2	9.5	10	5.4
3	14.5	8	4
4	6	10	4.5

The location of the origin of the coordinate system can be observed from the 3D image in Figure 6.

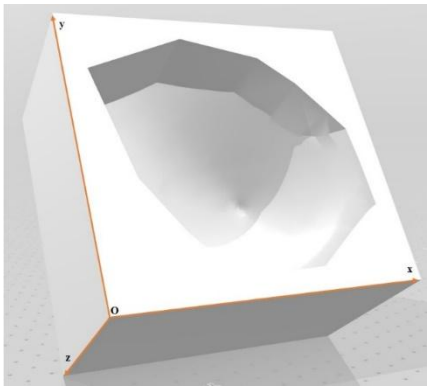

Figure 6. *3D image of the Mold with reference point*

2.3. Molding of silicone breasts

In this experiment, a 3D printer, called ZPrinter 450, is used to print the mold for casting silicone breasts (see Figure 7). This model has very high printing speed and allows printing objects of intricate shapes.

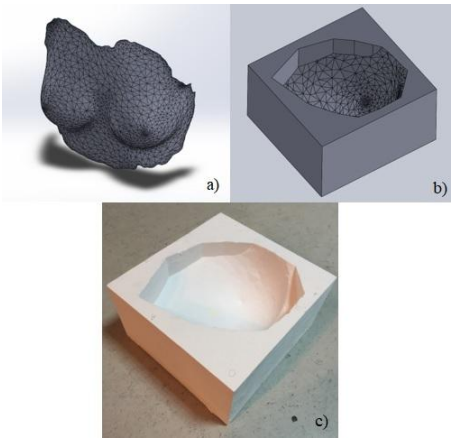

Figure 7. Mold printing: (a) scanned image by ZScanner 700; (b) 3D image of the mold created in Solidworks; (c) Mold manufactured by the 3D printer

The Dragon Skin 10 MEDIUM Set Silicone Rubber is used for casting breasts. One package of silicone rubber contains two ingredients, which should be properly mixed with a ratio of 1:1. The heat source made from resistors and wires is placed inside the mold at proper position, whose X, Y and Z coordinates should be recorded before the mixture is poured into the mold. Afterwards, the liquid silicone inside the mold is left for curing at room temperature for 4-6 hours. Finally, the prepared silicone breast is released from the mold. No releasing agent is required while using Dragon Skin 10 MEDIUM Set Silicone Rubber. The final breasts can be seen in Figure 8.

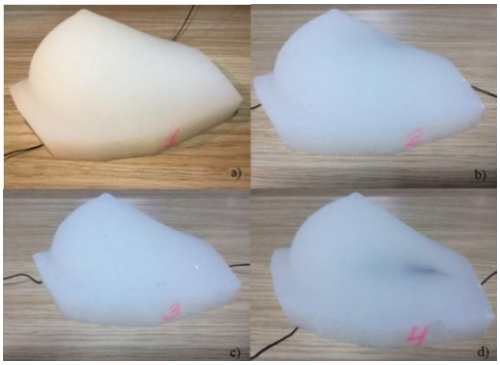

Figure 8. Silicone Breasts: (a) with a tumor size of 75.4 mm^3; (b) with a tumor size of 150.8 mm^3; (c) with a tumor size of 113.1 mm^3; (d) with a tumor size of 75.4 mm^3

2.4. Experimental procedure

The aim of the experiment was to take IR images of the silicone breast with the heat source inside by using the infrared camera and record the highest temperature value on the surface of the breast. At the beginning of the experiment, all the necessary equipment should be tested to ensure that they are in good working order before use. In addition, safety measures should be taken in order to prevent accidents or injuries during the experiment. Afterwards, the breast's initial temperature, room temperature and the temperature of the desk on which the silicone breast is placed should be measured by using the infrared camera. The room temperature should be held approximately at 24-26^{o}C. Moreover, the initial temperature of the breast has to be very close to the room temperature and to the temperature of the desk to be sure that ambient temperature will not significantly affect the temperature of the breast. Otherwise significant temperature differences can lead to significant convection heat transfer, causing the temperature of the breast to become unstable over time. Thermographic images are taken by the infrared camera and maximum temperature values are recorded after the power supply is turned on. Measurements will be taken every fifteen minutes.

3. Results and discussion

3.1. Silicone breast with a 75.4 mm^3 tumor size

The first experiment is done on the silicone breast with a *75.4 mm^3* tumor size. The heat source imitating a tumor inside the breast is located at the following coordinates: *x=9.2 cm, y=8.9 cm, z=3.5 cm*. The thermograms of the breast are shown below in Figure 9, where the presence of the heat source inside the breast can be clearly noticed from Figure 9 (d). The region with relatively hot temperature is located exactly on the top of the heat source and indicated by green color.

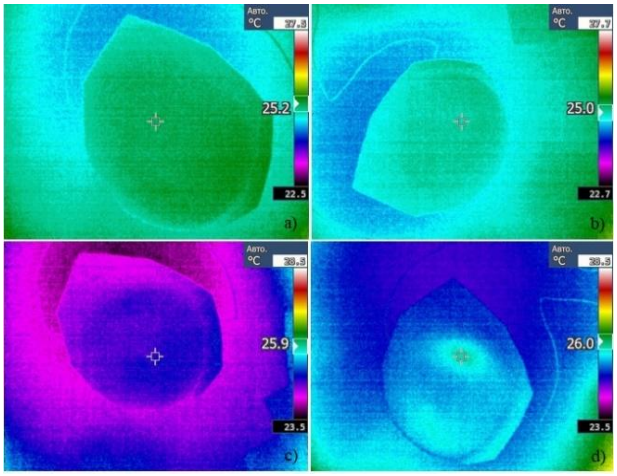

Figure 9 (a) infrared imaging for P=0.0027 W; (b) infrared imaging for P=0.01608 W; (c) infrared imaging for P=0.064 W; (d) infrared imaging for P=0.25408 W.

The current and voltage values for the resistors are given in Table 3. Maximum temperature values with respect to power output values given are also provided in the table.

Table 3. Data recorded with increase in power output in every 15 minutes

№	Voltage, V	Current, A	Power Output, W	Temperature, ℃
1	0	0	0	25.1
2	0.90	0.003	0.0027	25.2
3	2.01	0.008	0.01608	25.0
4	4.00	0.016	0.064	25.9
5	7.94	0.032	0.25408	26.0

It is very important to record the room temperature and the temperature of the desk on which the breast is placed (T_{room}=24.5 ℃, T_{desk}=24.4 ℃). If the ambient temperature is very low, it becomes very difficult to increase the temperature of the breast, thus leading to inaccurate results. For instance, the maximum temperature dropped from 25.2 ℃ to 25 ℃ despite a significant increase in the power output from 0.0027 W to 0.01608 W. The effect of the heat source on the temperature of the breast surface can be viewed from Figure 10. Although there is an slight initial drop in the temperature with a power value of 0.01608 W, the overall trend goes up.

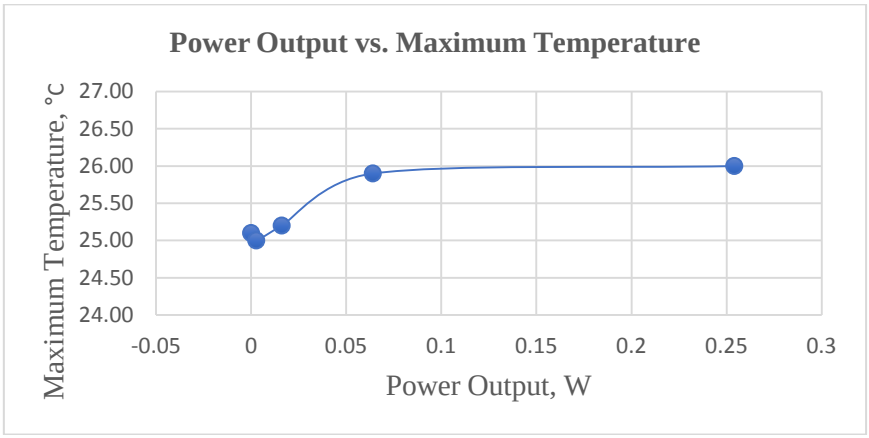

Figure 10. Power Output vs. Maximum Temperature

3.2. Silicone breast with a150.8 mm³ tumor size

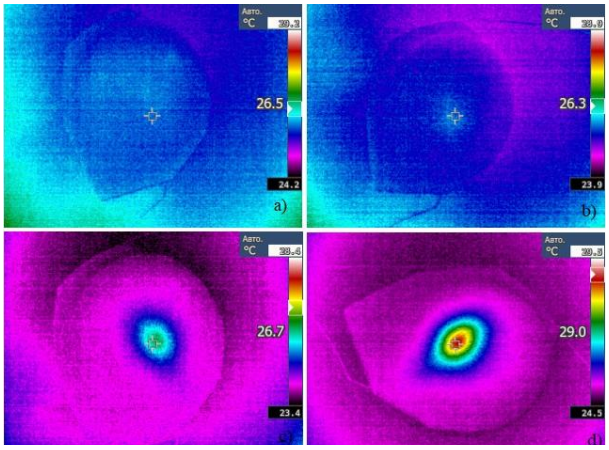

Figure 11. (a) infrared imaging for P=0.0081 W; (b) infrared imaging for P=0.02 W; (c) infrared imaging for P=0.09918 W; (d) infrared imaging for P=0.23085 W

The second experiment is conducted on the silicone breast with a *150.8 mm*^{3} tumor size. The heat source is located at the following location: *x=9.5 cm, y=10 cm, z=5.4 cm*. The thermograms of the breast are provided below in Figure 11. In Figure 11 (a), there is no observable presence of hotspot, but the general temperature of the surface is higher than its initial value. As the power output increases, the hot spot starts to form in Figure 11 (b). The presence of the heat source inside the breast can be clearly identified in Figure 11 (c) and (d). The region with relatively hot temperature is located exactly on the top of the heat source and indicated by red color. Temperature drop as it goes far from the hotspot can be observed from the different color layers around the hotspot. In this case, the presence of the heat source is very clear, since it is located close to the surface of the silicone breast.

The values of the voltage, current and measured maximum temperature are provided in Table 4.

Table 4. Values recorded with increase in the power output in every 15 minutes

№	Voltage, V	Current, A	Power Output, W	Temperature, ℃
1	0	0	0	25.6
2	1.62	0.005	0.0081	26.5
3	2.50	0.008	0.02	26.3
4	5.51	0.018	0.09918	26.7
5	8.55	0.027	0.23085	29.0

The room temperature and the temperature of the desk on which the breast is placed are T_{room}=24.8 ℃ and T_{desk}=25.6 ℃, respectively. Under these circumstances, the maximum temperature dropped from 26.5 ℃ to 26.3 ℃ despite the increase in the power output value from 0.0081 W to 0.02 W. The effect of the heat source on the surface temperature of the breast can be observed in Figure 12. Although, there is a drop in the temperature at the power value of 0.02 W initially, the overall temperature increases with power output.

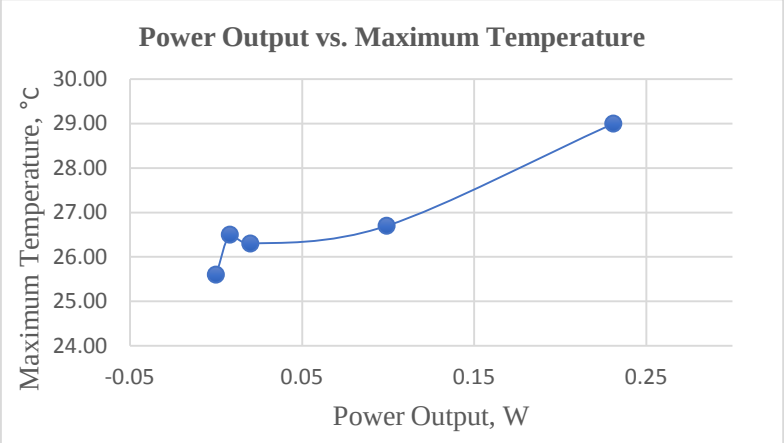

Figure 12. Power Output vs. Maximum Temperature

3.3. Silicone breast with a 113.1 mm^3 *tumor size*

The third experiment is undertaken on the silicone breast with a *113.1 mm*^{3} tumor size. The heat source imitating the tumor inside the breast is located at the following coordinates: *x=14.5 cm, y=8 cm, z=4 cm*. The thermograms of the breast are presented in Figure 13. In Figure 13 (a), there is no observable presence of hotspot, but the general temperature of the surface higher than on initial. From Figures 13 (b) and (c), it can be seen that the surface temperature increases with increment of power output. The presence of the heat source inside the breast can be clearly seen in Figure 13 (d), when the power output is high. The region with relatively hot temperature is located exactly on the top of heat source and indicated by light green and yellowish green color.

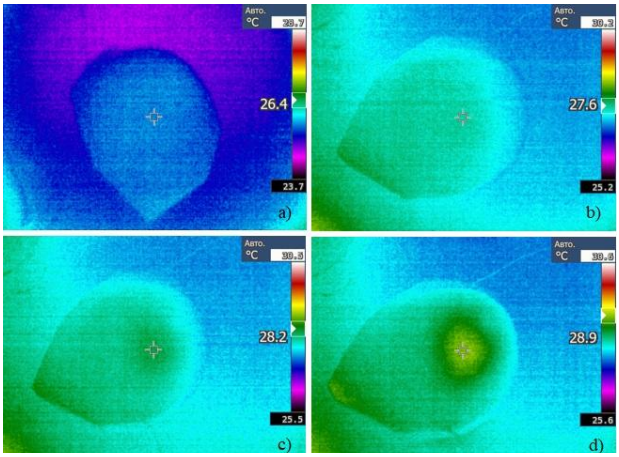

Figure 13. (a) infrared imaging for P=0.00486 W; (b) infrared imaging for P=0.0459 W; (c) infrared imaging for P=0.18685 W; (d) infrared imaging for P=0.42224 W

The voltage, current and measured maximum temperature values are given in Table 5.

Table 5. Values recorded with increase in power output in every 15 minutes

№	Voltage, V	Current, A	Power Output, W	Temperature, ℃
1	0	0	0	26.3
2	0.81	0.006	0.00486	26.4
3	2.55	0.018	0.0459	27.6
4	5.05	0.037	0.18685	28.2
5	7.54	0.056	0.42224	28.9

The room temperature and the temperature of the desk are T_{room}=26.3 ℃ and T_{desk}=26.3 ℃, respectively. The effect of the heat source on the maximum temperature of the breast surface can be examined in Figure 14, where it can be noticed that there is only a rising trend without any temperature drop.

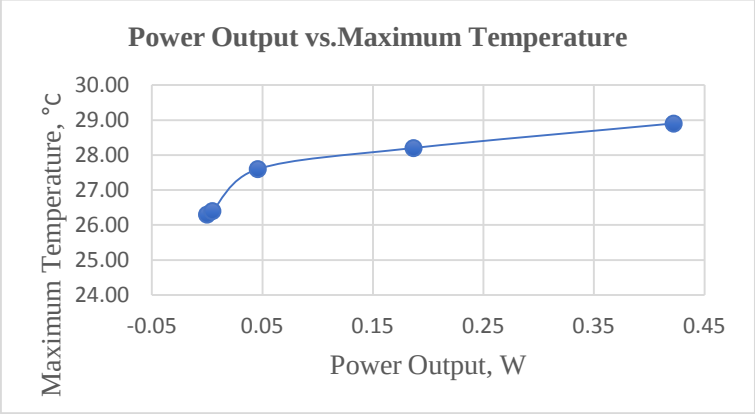

Figure 14. Power Output vs. Maximum Temperature

3.4. Silicone breast with a 75.4 mm^3 tumor size

The fourth experiment is done on the silicone breast with a *75.4 mm^3* tumor size. The heat source inside the breast is located at the following coordinates: *x=6 cm, y=10 cm, z=4.5 cm*. The thermograms of the breast are shown in Figure 15, where the presence of the heat source inside the breast can be noticed from Figures 15 (a) and (b). In Figures (c) and (d) the hotspot is clearly seen

with red color. Again the region with relatively hot temperature is located exactly on the top of heat source and indicated by red color.

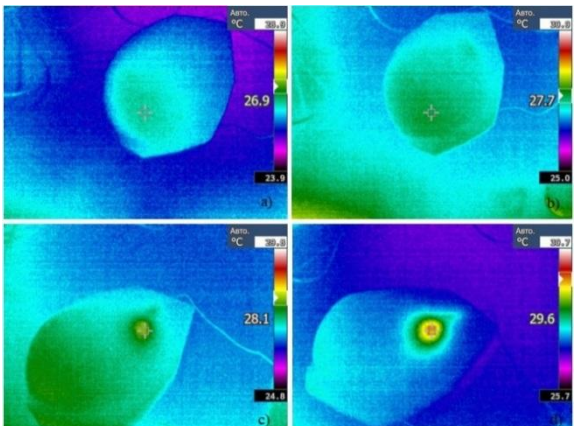

Figure 15. (a) infrared imaging for P=0.00297 W; (b) infrared imaging for P=0.01592 W; (c) infrared imaging for P=0.05012 W; (d) infrared imaging for P=0.16848 W

The recorded power output and maximum temperature values can be found from in Table 6 below.

Table 6. Values recorded with increase in power output in every 15 minutes

№	Voltage, V	Current, A	Power Output, W	Temperature, ℃
1	0	0	0	26.1
2	0.99	0.003	0.00297	26.9
3	1.99	0.008	0.01592	27.7
4	3.58	0.014	0.05012	28.1
5	6.48	0.026	0.16848	29.6

The room temperature and the temperature of the desk are T_{room}=25.8 ℃ and T_{desk}=26.3 ℃. The effect of the heat source on the temperature of the breast surface can analysed from Figure 16. It can be noticed from the graph that there is only an upward trend without any temperature drop. Significant temperature rises are observed for power output values of 0.00297 W, 0.01592 W and 0.05012 W.

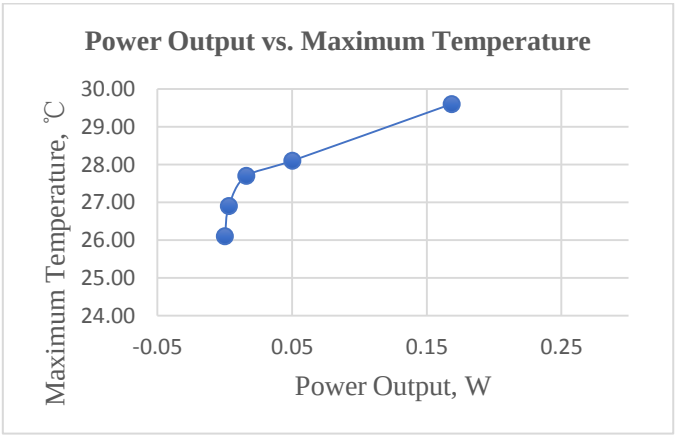

Figure 16. Power Output vs. Maximum Temperature

3.5. Comparison of temperature profiles

Combining all of the graphs in Figure 17, representing the effect of the increase of the power output on the temperature profile, it becomes clear that the maximum temperature values of the third and fourth breasts are going exclusively up as the given value of the power output increases. However, the graphs showing the temperature profiles of another two breasts have negligible temperature drops after

increasing the power to the second values, but then temperature goes up again. This is due to the reason that the temperature inside the room where the experiment is conducted is lower compared to the initial surface temperature of the breast. Accordingly, convection heat transfer takes place. But when sufficient amount of power is given to the circuit temperature will start to grow. It can also be noticed that for the second case where the tumor has a size of $150.8\ mm^3$, the magnitude of the temperature is sharply going up, while for the first case where the tumor size is $75.4\ mm^3$ the temperature is increasing gradually. Overall, the temperature increases sharply for the second and fourth cases, since for both cases the tumor is located very close to the surface of the breast and thus showing clear temperature difference on the thermograms provided. In the other two cases, the tumors are located deep inside the breasts, therefore temperature increases on the surfaces of the breasts are at moderate rate.

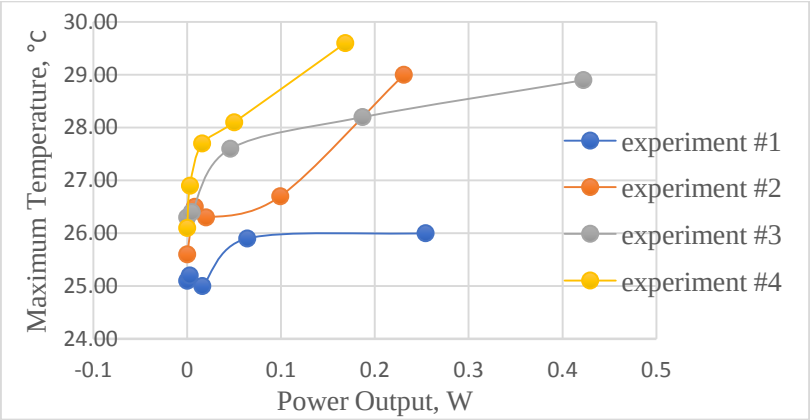

Figure 17. Power Output vs. Maximum temperature

4. Conclusion and future work

Overall the main purpose of this study is to develop an experimental procedure in order to generate experimental results for FEM model validation. The breast of a female mannequin is used as a breast model, which is scanned and its replicas are produced by 3D printing the mold and molding it with silicon. The molded breasts are fitted with resistor heaters as models of tumors. IR imaging and temperature measurements are then taken in the experiment with an accuracy of 0.1 degree in temperature. The results from the experiment are successfully generated and can be used for the validation of FEM simulations.

For future work, FEM thermal models and simulations will be validated with the data obtained in this study. Furthermore, breast cancer patients' data will be obtained using the same procedure with 3D scanning and IR imaging. A toolbox will be developed incorporating a FEM code for inverse thermal modeling based on a search scheme and the patients' data to search for the sizes and locations of tumors in the patients' breasts.

References

[1] Francis, S. V., Sasikala, M., & Jaipurkar, S. D. (2017). Detection of Breast Abnormality Using Rotational Thermography. In *Application of Infrared to Biomedical Sciences* (pp. 133-158). Springer Singapore.

[2] HealthGrove. (2013). Breast Cancer in Kazakhstan. Retrieved November 15, 2017, from http://global-disease-burden.healthgrove.com/l/33097/Breast-Cancer-in-Kazakhstan.

[3] Sejtkazina, G. D., Bajpeisov, D. M., Sejsenbaeva, G. T., & onkologicheskoj sluzhby Respubliki, A. A. P. (2012). Kazahstan za 2011 god (statisticheskie materialy) (Indicators Oncology Service of the Republic of Kazakhstan for 2013 (statistical material)).

[4] Toleutay, U., Reznik, V., Kalmatayeva, Z., & Smigelskas, K. (2013). Risk factors of breast cancer in Kyzylorda oblast of Kazakhstan: a case-control study. *Asian Pacific Journal of Cancer Prevention*, *14*(10), 5961-5964.

[5] Bilyalova, Z., Igissinov, N., Moore, M., Igissinov, S., Sarsenova, S., & Khassenova, Z. (2012). Epidemiological evaluation of breast cancer in ecological areas of Kazakhstan-association with pollution emissions. *Asian Pacific Journal of Cancer Prevention*, *13*(5), 2341-2344.

[6] Keyserlingk, M. D. (1998). *Infrared Imaging of the Breast: Initial Reappraisal Using High-Resolution Digital Technology in 100 successive cases of Stage I and II Breast Cancer*(Vol. 4, pp. 245-251, Publication). The Breast Journal.

[7] Jiang, L. J., Ng, E. Y. K., Yeo, A. C. B., Wu, S., Pan, F., Yau, W. Y., ... & Yang, Y. (2005). A perspective on medical infrared imaging. *Journal of medical engineering & technology*, *29*(6), 257-267.

[8] Gautherie, M. (1989). Atlas of breast thermography with specific guidelines for examination and interpretation. *Milan, Italy: PAPUSA*, *256*.

[9] Acharya, U. R., Ng, E. Y. K., Tan, J. H., & Sree, S. V. (2012). Thermography based breast cancer detection using texture features and support vector machine. *Journal of medical systems*, *36*(3), 1503-1510.

[10] Hoekstra P, The autonomic challenge and analytic breast thermology. Thermology International, 2004(14);3:106.

[11] Kennedy, D. M., Lee, T., & Seely, D. (2009). *A Comparative Review of Thermography as a Breast Cancer Screening Technique*(1st ed., Vol. 8, pp. 9-16, Publication). Toronto, Ontario, Canada: The Canadian College of Naturopathic Medicine. doi:10.1177/1534735408326171